Journal Applied Science and Technology on Naval Engineering
e-ISSN: 3031-8866

Ship Manuvering Analysis Using Virtual Captive Model Test On Trim And Sinkage Variations

Audi Razif Santoso[1,*], Fakhri Akbar Ayub[1]

[1]Naval Architecture, Universitas Pembangunan Nasional Veteran Jakarta, Jakarta, 16514, Indonesia
*Corresponding author: 2110313029@mahasiswa.upnvj.ac.id

Received: 06/07/2026; Revised: 07/08/2026; Accepted: 10/08/2026; Published: 14/08/2026
Vol. 4, No. 2, August 2026, pp. 39-48
DOI: https://doi.org/10.54378/astne.v4i2.05

Abstract

This study evaluates the effect of trim and sinkage variations on ship hydrodynamic characteristics using the Virtual Captive Model Test (VCMT) based on Computational Fluid Dynamics (CFD) for the KRISO Container Ship (KCS) model. Simulations were conducted for sinkage variations of −0.00090, −0.00275, and −0.00599 and trim variations of 0.017°, 0.053°, and 0.097°, over drift angles ranging from 2° to 10° under two speed conditions represented by Froude numbers 0.152 and 0.163. The objective is to investigate the influence of trim and sinkage on lateral force (sway) and yaw moment and to determine hydrodynamic coefficients using the Least Squares regression method. The results show that trim and sinkage influence sway force and yaw moment, although their effects are smaller than those of speed and drift angle. Increased sinkage generally produces higher sway force and yaw moment due to increased wetted surface area and changes in hull pressure distribution, while trim mainly alters the longitudinal pressure distribution with relatively limited influence within the investigated range. The maximum nondimensional values of Y′ and N′ were obtained at Fr = 0.163 and a drift angle of 10° (Y′H = 0.206543 and N′H = 0.079192 for sinkage variation; Y′H = 0.202338 and N′H = 0.073965 for trim variation). The hydrodynamic forces and moments were nondimensionalized using the Yoshimura–Masumoto formulation and analyzed through Least Squares regression, yielding coefficients that agree well with the simulation results. The VCMT-based CFD approach combined with Least Squares regression provides an effective alternative for determining ship maneuvering hydrodynamic coefficients.

Keywords: Virtual Captive Model Test; Computational Fluid Dynamic; Trim; Sinkage; Sway Force;

1. Introduction

Ship maneuverability is an essential aspect of ship design because it determines a vessel's ability to maintain course, change direction, and operate safely under various environmental conditions. Accurate prediction of maneuvering performance is required to ensure navigation safety and compliance with the maneuverability standards established by the International Maritime Organization (IMO, 2002). The maneuvering behavior of a ship is governed by hydrodynamic forces and moments acting on the hull, propeller, and rudder, which are commonly represented by hydrodynamic coefficients in mathematical maneuvering models such as the Maneuvering Modeling Group (MMG) model (Yasukawa & Yoshimura, 2015). Therefore, obtaining reliable hydrodynamic coefficients is an important step in ship maneuvering analysis.

Conventionally, hydrodynamic coefficients are determined through captive model tests, such as the Planar Motion Mechanism (PMM) test. Although these experimental methods provide reliable results, they require specialized facilities, physical ship models, and considerable testing time and cost (Kim et al., 2022). Recent advances in Computational Fluid Dynamics (CFD) have enabled the development of the Virtual Captive Model Test (VCMT), which numerically reproduces captive tests and offers a more efficient alternative for estimating hydrodynamic forces and moments (Hajivand & Mousavizadegan, 2015; Kim et al., 2022). In addition, hydrodynamic coefficients obtained from CFD simulations can be identified using the Least Squares regression method, which has been widely applied to derive maneuvering coefficients from numerical and experimental data (Papanikolaou, 2014).

The application of Computational Fluid Dynamics (CFD) in ship maneuvering analysis has developed significantly in recent years, particularly through the implementation of the Virtual Captive Model Test (VCMT). Hino (2015) demonstrated that CFD-based captive model tests can accurately predict hydrodynamic forces and moments for maneuvering analysis. Carrica et al. (2016) further highlighted the capability of CFD to simulate complex maneuvering motions with reasonable accuracy, while Liu et al. (2018) reported that hydrodynamic derivatives obtained from CFD show good agreement with experimental results. In addition, Du et al. (2022) successfully integrated VCMT with the MMG mathematical model to determine maneuvering hydrodynamic coefficients, confirming the reliability of CFD-based approaches for maneuvering prediction.

Previous studies have successfully applied VCMT to investigate the effects of drift angle and ship speed on maneuvering hydrodynamic characteristics. However, the influence of trim and sinkage has received relatively limited attention, even though both parameters alter the underwater hull geometry, wetted surface area, and pressure distribution around the hull, thereby affecting the generated sway force and yaw moment (Shivachev et al., 2017; Molland et al., 2017). To address this gap, this study investigates the influence of trim and sinkage variations on the maneuvering characteristics of the KRISO Container Ship (KCS) model using VCMT based on CFD under different drift angles and Froude numbers.

The hydrodynamic forces and moments obtained from the simulations are nondimensionalized using the Yoshimura Masumoto formulation (Yoshimura & Masumoto, 2012), and the corresponding hydrodynamic coefficients are identified using the Least Squares regression method. This study integrates VCMT-based CFD simulations with trim and sinkage variations to evaluate their influence on sway force, yaw moment, and maneuvering hydrodynamic coefficients. The results are expected to provide a practical and cost-effective approach for determining hydrodynamic coefficients while improving the understanding of trim and sinkage effects on ship maneuvering performance.

This paper is organized as follows. Section 2 describes the research methodology, including the computational model, numerical simulation, and hydrodynamic coefficient identification. Section 3 presents and discusses the simulation results. Finally, Section 4 concludes the main findings of this study.

2. Methodology

2.1 Ship Model

The ship model used in this study was the KRISO Container Ship (KCS), which is widely adopted as a benchmark for ship hydrodynamic and maneuvering research (Khan et al., 2022). A model scale of 1:31.5 was applied, resulting in a model length between perpendiculars (Lpp) of 7.27 m, beam (B) of 1.01 m, and draft (T) of 0.34 m. Three sinkage conditions (−0.00090 m, −0.00275 m, and −0.00599 m) and three trim conditions (0.017°, 0.053°, and 0.097°) were investigated. Simulations were performed at two operating speeds corresponding to Froude numbers of 0.152 and 0.163, with drift angles ranging from 2° to 10°.

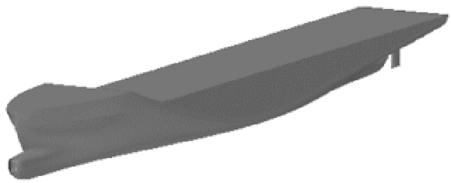

Figure 1. Ship Model

2.2 Numerical Simulation (CFD)

The numerical simulations were carried out using CFD. A pressure-based steady-state solver with the k–ω SST turbulence model was employed because of its capability to accurately predict flow separation and near-wall flow behavior. The Volume of Fluid (VOF) method was used to model the free surface between water and air. The computational domain followed the ITTC recommendations, and the ship surface was defined as a no-slip wall. Mesh independence was evaluated using several mesh densities, and approximately one million cells were selected because they provided stable convergence and satisfactory agreement with reference drag coefficient data.

The computational domain was established according to the ITTC recommendations. The domain extended from −1.0 Lpp to 4.0 Lpp in the longitudinal direction (X-axis), −1.5 Lpp to 1.5 Lpp in the transverse direction (Y-axis), and −1.0 Lpp to 0.5 Lpp in the vertical direction (Z-axis), providing sufficient space to minimize boundary effects during the CFD simulations.

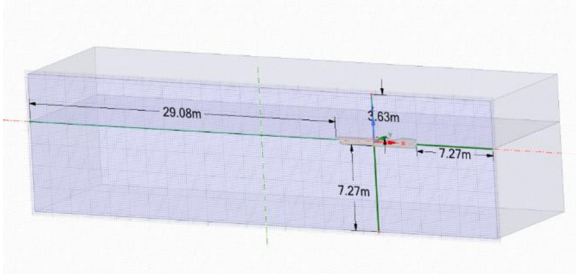

Figure 2. Enclosure

2.3 Model Validation

A mesh independence study was conducted using several mesh densities to ensure numerical stability. The simulation results were validated by comparing the drag coefficient obtained from CFD with the available experimental data. The mesh consisting of approximately one million cells was selected because it provided stable convergence and the closest agreement with the reference drag coefficient, with an error below 5% for most operating conditions. The corresponding mesh independence and validation results are summarized in Table 1 and illustrated in Figure 3.

Table 1. Grid Independence Test

VS	EFD	CFD 800000 Mesh	CFD 900000 Mesh	CFD 1000000 Mesh
0.915	3.796	3.882	3.835	3.611
1.647	3.475	3.590	3.585	3.350
2.196	3.711	3.553	3.533	3.532

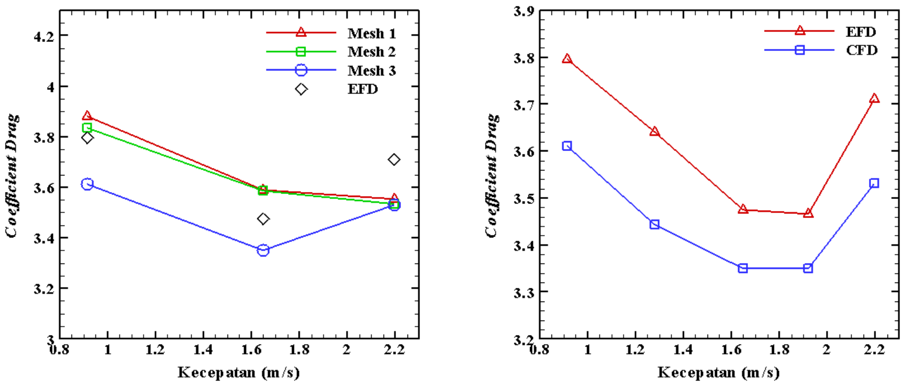

Figure 3. (a) Comparison of Drag Coefficients for Different Mesh Densities (b)Speed Validation

2.4 Virtual Captive Model Test

The Virtual Captive Model Test (VCMT) was carried out using the static drift method. The ship model was fixed at drift angles of 2°, 4°, 6°, 8°, and 10° while maintaining constant forward speed. Simulations were performed for each trim and sinkage variation under Froude numbers of 0.152 and 0.163. The resulting lateral force (Y) and yaw moment (N) obtained from each simulation were used for further hydrodynamic analysis. Representative velocity contours for the sinkage and trim conditions are shown in Figure 4.

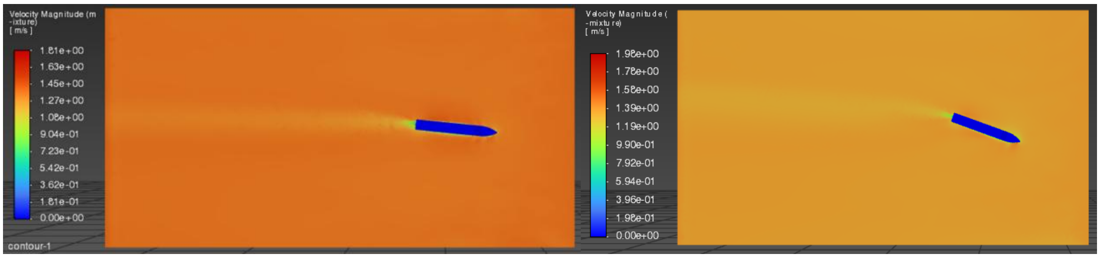

Figure 4. (a) VCMT for Sink Condition (b) VCMT for Trim Condition

2.5 Hydrodynamic Coefficient Identification

The hydrodynamic coefficients were determined from the CFD results through three stages: conversion of drift angle, non-dimensionalization of hydrodynamic forces, and Least Squares regression.

The drift angle was first converted from degrees to radians using:

$$\beta_{rad} = \beta_{deg} \times \frac{\pi}{180} \tag{1}$$

The non-dimensional lateral velocity was then calculated as:

$$v' = sin\beta \tag{2}$$

where v' is the non-dimensional lateral velocity and β is the drift angle in radians.

The lateral force and yaw moment obtained from the CFD simulations were converted into non-dimensional hydrodynamic coefficients using the Yoshimura–Masumoto formulation (Yoshimura & Masumoto, 2012):

$$Y_H = \frac{Y(CFD)}{\frac{1}{2}\rho U^2 LT} \tag{3}$$

$$N_H = \frac{N(CFD)}{\frac{1}{2}\rho U^2 L^2 T} \tag{4}$$

where

- Y= lateral force (N)
- N= yaw moment (N·m)
- ρ= water density (kg/m³)
- U= ship velocity (m/s)
- L_{pp}= length between perpendiculars (m)
- T= ship draft (m)

The Least Squares (LSQ) method was employed to determine the maneuvering hydrodynamic derivatives from the CFD simulation results. The regression coefficients were calculated using the matrix formulation presented in Equation (5), where X denotes the matrix of independent variables, Y represents the vector of observed hydrodynamic responses, and β is the vector of regression coefficients obtained by minimizing the sum of squared residuals.

$$\beta = (X^T X)^{-1} X^T Y \quad (5)$$

The hydrodynamic coefficients were identified using the Least Squares (LSQ) regression method and than applied based on a third-order polynomial model:

$$Y'_H = av' + bv'^3 \quad (6)$$

$$N'_H = av' + bv'^3 \quad (7)$$

where a and b are the hydrodynamic derivatives determined by the Least Squares regression.

3. Results and Discussion

The effects of trim and sinkage variations on the hydrodynamic characteristics of the KRISO Container Ship (KCS) model were investigated through Virtual Captive Model Test (VCMT) simulations under different drift angles and Froude numbers. The obtained lateral force (sway force) and yaw moment were analyzed to evaluate the influence of trim and sinkage on ship maneuvering performance.

The VCMT results presented in Tables (2) show that sway force and yaw moment increase with increasing drift angle and Froude number. The highest values were obtained at Fr = 0.163 and 10° drift angle, while the lowest occurred at Fr = 0.152 and 2° drift angle. Although trim and sinkage have a smaller influence than drift angle and ship speed, both parameters modify the hydrodynamic response by changing the pressure distribution and wetted surface area around the hull.

Table 2. VCMT Result on Y and N

FR	Drift	Trim	Y	N	Sink	Y	N
1.279	4	0.017 °	36.1842	181.5603	−0.00090	10.0062	66.4956
1.279	6	0.017 °	58.9375	240.5615	−0.00090	38.3152	194.8274
1.279	8	0.017 °	175.3289	538.4512	−0.00090	116.5555	402.1790
1.279	10	0.017 °	349.7668	946.6723	−0.00090	242.6778	715.3920
1.279	2	0.053 °	8.5727	61.8499	−0.00090	432.3860	1200.3145
1.279	4	0.053 °	38.2716	184.1116	−0.00275	10.5175	66.63090
1.279	6	0.053 °	61.2569	247.6972	−0.00275	39.3255	197.80860
1.279	8	0.053 °	172.4727	494.4343	−0.00275	47.0591	406.20490
1.279	10	0.053 °	353.8052	943.5137	−0.00275	244.7012	719.30430
1.279	2	0.097 °	10.0244	63.1883	−0.00275	433.9587	1,202.97510
1.279	4	0.097 °	36.7725	178.1498	−0.00599	11.2618	68.0655
1.279	6	0.097 °	114.4756	376.9865	−0.00599	39.4525	200.4591
1.279	8	0.097 °	237.8602	654.3342	−0.00599	118.6445	414.4391
1.279	10	0.097 °	423.3985	1,094	−0.00599	247.7875	731.1705
1.376	2 °	0.017 °	8.1322	62.9556	−0.00090	11.4039	74.2123
1.376	4 °	0.017 °	43.8413	203.7722	−0.00090	44.0388	225.4778
1.376	6°	0.017 °	68.4847	270.4899	−0.00090	135.5449	465.4966
1.376	8°	0.017 °	204.4674	585.6489	−0.00090	279.7179	828.9030
1.376	10°	0.017 °	397.4854	1041.9530	−0.00090	497.7884	1391.4865
1.376	2 °	0.053 °	10.0229	70.9136	−0.00275	12.9069	70.3404
1.376	4 °	0.053 °	43.8788	213.3831	−0.00275	45.2678	214.7942
1.376	6°	0.053 °	70.2851	287.8648	−0.00275	131.0125	442.6378
1.376	8°	0.053 °	201.4116	613.6378	−0.00275	286.3957	812.2021
1.376	10°	0.053 °	393.7630	1022.0064	−0.00275	476.2925	1292.8421
1.376	2 °	0.097 °	11.5904	72.9982	−0.00599	13.1735	78.3574
1.376	4 °	0.097 °	42.1748	205.8919	−0.00599	45.3137	232.5116
1.376	6°	0.097 °	132.4916	435.7840	−0.00599	138.3667	479.8866

1.376	8°	0.097 °	273.2627	759.6517	−0.00599	285.2939	847.3317
1.376	10°	0.097 °	488.4599	1299.6374	−0.00599	498.6113	1389.7256

Following the CFD simulations, the hydrodynamic forces and moments were converted into nondimensional coefficients using the Yoshimura–Masumoto formulation. Tables (3) show that the conversion preserved the overall trend of the data while eliminating the scale effect, allowing the coefficients to be used for hydrodynamic derivative identification.

Table 3. Conversion Result on YH and NH

Rad	V'	V'3	Drift	Trim	YH	NH	Sink	YH	NH
0.03491	0.03490	0.00004	4	0.017 °	0.003697	0.003696	−0.00090	0.004797	0.004380
0.06981	0.06976	0.00034	6	0.017 °	0.017349	0.011960	−0.00090	0.018370	0.012834
0.10472	0.10453	0.00114	8	0.017 °	0.028258	0.015846	−0.00090	0.055883	0.026492
0.13963	0.13917	0.00270	10	0.017 °	0.084062	0.035469	−0.00090	0.116352	0.047124
0.17453	0.17365	0.00524	2	0.053 °	0.167696	0.062359	−0.00090	0.207308	0.079066
0.03491	0.03490	0.00004	4	0.053 °	0.004110	0.004074	−0.00275	0.005043	0.004389
0.06981	0.06976	0.00034	6	0.053 °	0.018349	0.012128	−0.00275	0.018855	0.013030
0.10472	0.10453	0.00114	8	0.053 °	0.029370	0.016316	−0.00275	0.022563	0.026757
0.13963	0.13917	0.00270	10	0.053 °	0.082692	0.032569	−0.00275	0.117322	0.047382
0.17453	0.17365	0.00524	2	0.097 °	0.169633	0.062151	−0.00275	0.208062	0.079242
0.03491	0.03490	0.00004	4	0.097 °	0.004806	0.004162	−0.00599	0.005399	0.004484
0.06981	0.06976	0.00034	6	0.097 °	0.017631	0.011735	−0.00599	0.018916	0.013205
0.10472	0.10453	0.00114	8	0.097 °	0.054886	0.024833	−0.00599	0.056884	0.027300
0.13963	0.13917	0.00270	10	0.097 °	0.114043	0.043102	−0.00599	0.118802	0.048163
0.17453	0.17365	0.00524	2 °	0.017 °	0.003369	0.003583	−0.00090	0.004724	0.004224
0.03491	0.03490	0.00004	4 °	0.017 °	0.018161	0.011597	−0.00090	0.018243	0.012832
0.06981	0.06976	0.00034	6°	0.017 °	0.028369	0.015394	−0.00090	0.056148	0.026492
0.10472	0.10453	0.00114	8°	0.017 °	0.084698	0.033330	−0.00090	0.115870	0.047174
0.13963	0.13917	0.00270	10°	0.017 °	0.164653	0.059299	−0.00090	0.206203	0.079192
0.17453	0.17365	0.00524	2 °	0.053 °	0.004152	0.004036	−0.00275	0.005347	0.004003
0.03491	0.03490	0.00004	4 °	0.053 °	0.018176	0.012144	−0.00275	0.018752	0.012224
0.06981	0.06976	0.00034	6°	0.053 °	0.029115	0.016383	−0.00275	0.054270	0.025191
0.10472	0.10453	0.00114	8°	0.053 °	0.083432	0.034923	−0.00275	0.118636	0.046224
0.13963	0.13917	0.00270	10°	0.053 °	0.163111	0.058164	−0.00275	0.197298	0.073578
0.17453	0.17365	0.00524	2 °	0.097 °	0.004801	0.004154	−0.00599	0.005457	0.004459
0.03491	0.03490	0.00004	4 °	0.097 °	0.017470	0.011718	−0.00599	0.018771	0.013233
0.06981	0.06976	0.00034	6°	0.097 °	0.054883	0.024801	−0.00599	0.057317	0.027311
0.10472	0.10453	0.00114	8°	0.097 °	0.113196	0.043233	−0.00599	0.118179	0.048223
0.13963	0.13917	0.00270	10°	0.097 °	0.202338	0.073965	−0.00599	0.206543	0.079092

The identified nondimensional coefficients were subsequently fitted using the LSQ regression method. The resulting regression constants, presented in Tables (4) , reveal the contribution of both linear and nonlinear components to the maneuvering characteristics.

Table 4. LSQ Results

Parameters	Sway	Yaw	Description
A	0.07643	0.11545	Linear
B	34.32566	9.81361	Non Linear

A comparison between the nondimensional coefficients and the LSQ regression results is presented in Tables 5 and 6. The fitted regression curves closely follow the CFD data, demonstrating that the LSQ method adequately represents the hydrodynamic behavior within the investigated drift angle range. The corresponding comparisons between the CFD data and the LSQ regression curves are illustrated in Figures 5 and 6.

Table 5. Comparison of Conversion and Regression Results Of Y'_H and N'_H on Trim Condition

Drift	Trim	Y'H Coversion	Y'H Regression	N'H Conversion	N'H Regression
4	0.017 °	0.003697	0.004126	0.003696	0.004446
6	0.017 °	0.017349	0.016983	0.011960	0.011384
8	0.017 °	0.028258	0.047192	0.015846	0.023276
10	0.017 °	0.084062	0.103167	0.035469	0.042522
2	0.053 °	0.167696	0.193005	0.062359	0.071433
4	0.053 °	0.004110	0.004126	0.004074	0.004446
6	0.053 °	0.018349	0.016983	0.012128	0.011384
8	0.053 °	0.029370	0.047192	0.016316	0.023276
10	0.053 °	0.082692	0.103167	0.032569	0.042522
2	0.097 °	0.169633	0.193005	0.062151	0.071433
4	0.097 °	0.004806	0.004126	0.004162	0.004446
6	0.097 °	0.017631	0.016983	0.011735	0.011384
8	0.097 °	0.054886	0.047192	0.024833	0.023276
10	0.097 °	0.114043	0.103167	0.043102	0.042522
2 °	0.017 °	0.003369	0.004126	0.003583	0.004446
4 °	0.017 °	0.018161	0.016983	0.011597	0.011384
6°	0.017 °	0.028369	0.047192	0.015394	0.023276
8°	0.017 °	0.084698	0.103167	0.033330	0.042522
10°	0.017 °	0.164653	0.193005	0.059299	0.071433
2 °	0.053 °	0.004152	0.004126	0.004036	0.004446
4 °	0.053 °	0.018176	0.016983	0.012144	0.011384
6°	0.053 °	0.029115	0.047192	0.016383	0.023276
8°	0.053 °	0.083432	0.103167	0.034923	0.042522
10°	0.053 °	0.163111	0.193005	0.058164	0.071433
2 °	0.097 °	0.004801	0.004126	0.004154	0.004446
4 °	0.097 °	0.017470	0.016983	0.011718	0.011384
6°	0.097 °	0.054883	0.047192	0.024801	0.023276
8°	0.097 °	0.113196	0.103167	0.043233	0.042522
10°	0.097 °	0.202338	0.193005	0.073965	0.071433

Table 6. Comparison of Conversion and Regression Results Of Y'_H and N'_H on Sink Condition

Drift	Sink	Y'H Coversion	Y'H Regression	N'H Conversion	N'H Regression
4	−0.00090	0.004797	0.004126	0.004380	0.004446
6	−0.00090	0.018370	0.016983	0.012834	0.011384
8	−0.00090	0.055883	0.047192	0.026492	0.023276
10	−0.00090	0.116352	0.103167	0.047124	0.042522
2	−0.00090	0.207308	0.193005	0.079066	0.071433
4	−0.00275	0.005043	0.004126	0.004389	0.004446
6	−0.00275	0.018855	0.016983	0.013030	0.011384
8	−0.00275	0.022563	0.047192	0.026757	0.023276
10	−0.00275	0.117322	0.103167	0.047382	0.042522
2	−0.00275	0.208062	0.193005	0.079242	0.071433
4	−0.00599	0.005399	0.004126	0.004484	0.004446

6	−0.00599	0.018916	0.016983	0.013205	0.011384
8	−0.00599	0.056884	0.047192	0.027300	0.023276
10	−0.00599	0.118802	0.103167	0.048163	0.042522
2 °	−0.00090	0.004724	0.193005	0.004224	0.004446
4 °	−0.00090	0.018243	0.004126	0.012832	0.011384
6°	−0.00090	0.056148	0.016983	0.026492	0.023276
8°	−0.00090	0.115870	0.047192	0.047174	0.042522
10°	−0.00090	0.206203	0.103167	0.079192	0.071433
2 °	−0.00275	0.005347	0.004126	0.004003	0.004446
4 °	−0.00275	0.018752	0.016983	0.012224	0.011384
6°	−0.00275	0.054270	0.047192	0.025191	0.023276
8°	−0.00275	0.118636	0.103167	0.046224	0.042522
10°	−0.00275	0.197298	0.193005	0.073578	0.071433
2 °	−0.00599	0.005457	0.004126	0.004459	0.004446
4 °	−0.00599	0.018771	0.016983	0.013233	0.011384
6°	−0.00599	0.057317	0.047192	0.027311	0.023276
8°	−0.00599	0.118179	0.103167	0.048223	0.042522
10°	−0.00599	0.206543	0.193005	0.079092	0.071433

The regression constants were subsequently substituted into the MMG hydrodynamic derivative equations to obtain the maneuvering coefficients. These derivatives describe the linear and nonlinear responses of sway force and yaw moment and provide the required input parameters for MMG-based maneuvering simulations.

$$Y'_H = 0{,}07643v' + 34{,}32566v'^3 \quad (8)$$

$$N'_H = 0{,}11545v' + 9{,}81361v'^3 \quad (9)$$

The identified hydrodynamic derivatives demonstrate the contribution of both linear and nonlinear components to the maneuvering behavior of the KCS model. The obtained coefficients can be directly implemented as input parameters in the MMG mathematical model for subsequent maneuvering simulations, including turning circle and zig-zag tests.

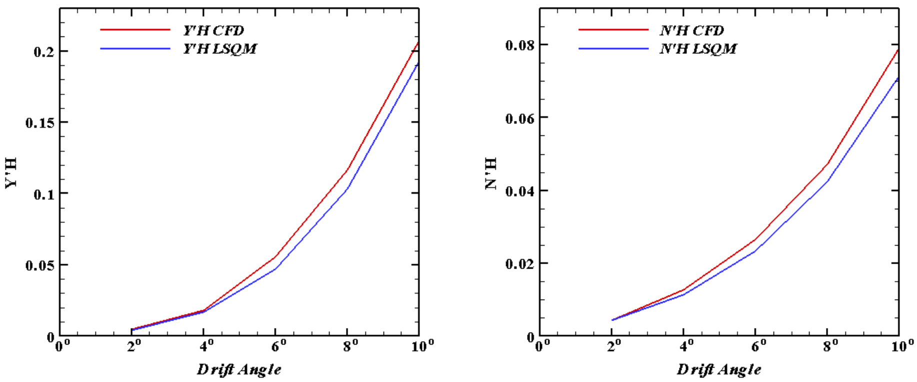

Figure 5. (a) Comparison of CFD and LSQ Regression Results for at a Sinkage of −0.00090 m (Vs = 1.279 m/s) (b) Comparison of CFD and LSQ Regression Results for at a Sinkage of −0.00090 m (Vs = 1.279 m/s)

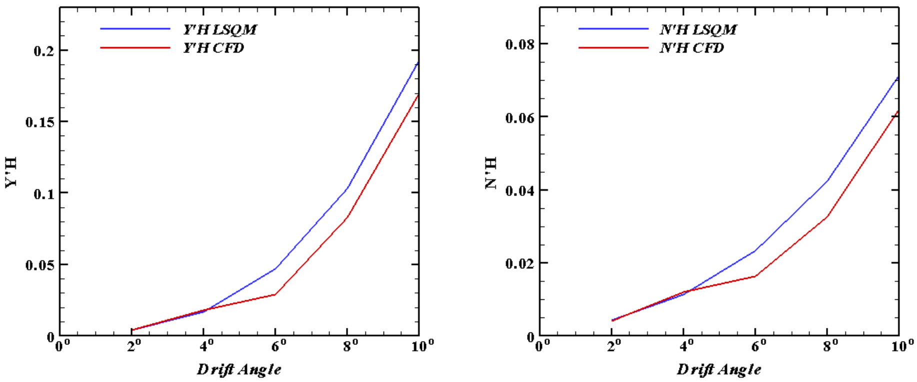

Figure 6. (a) Comparison of CFD and LSQ Regression Results for at a Trim of 0.053° (Vs = 1.279 m/s) (b) Comparison of CFD and LSQ Regression Results for at a Trim of 0.053° (Vs = 1.279 m/s)

4. Conclusion

The present study successfully applied the Virtual Captive Model Test (VCMT) based on Computational Fluid Dynamics (CFD) to evaluate the maneuvering characteristics of the KRISO Container Ship (KCS). The simulation results demonstrated that sway force and yaw moment were affected by drift angle, Froude number, trim, and sinkage. Among these parameters, drift angle and ship speed produced the most significant influence, while trim and sinkage modified the hydrodynamic response by altering the pressure distribution and wetted surface area around the hull.

The results further indicate that trim has a more pronounced effect on maneuvering hydrodynamic characteristics than sinkage within the investigated operating conditions. An increase in trim resulted in noticeable changes in sway force and yaw moment, whereas the influence of sinkage remained relatively small. These findings suggest that trim plays a more important role in modifying the hydrodynamic behavior of the KCS model during maneuvering.

Furthermore, the combination of nondimensionalization and the Least Squares (LSQ) regression method successfully identified the maneuvering hydrodynamic derivatives required by the MMG mathematical model. The obtained regression coefficients represent the relationship between nondimensional lateral velocity and the corresponding hydrodynamic forces and moments, providing reliable input parameters for future ship maneuvering simulations, including turning circle and zig-zag maneuvers.

References

Ayub, F. A., & Furukawa, Y. (2024). Comparison Between Cubic and Quadratic Models of Hydrodynamic Derivatives to the Ship Course Stability Index. *International Journal of Technology, 15*(5), 1502–1523. https://doi.org/10.14716/ijtech.v15i5.7036

Barr, R. A. (2016). *Ship Maneuvering and Control.* Springer.

Carrica, P. M., Wilson, R. V., Sadat-Hosseini, H., & Stern, F. (2016). CFD simulations of ship maneuvering: Past, present, and future. *Ocean Engineering, 116*, 1–18. https://doi.org/10.1016/j.oceaneng.2016.02.007

Chapra, S. C., & Canale, R. P. (2010). *Numerical Methods for Engineers* (6th ed.). McGraw-Hill.

Du, P., Liu, Z., & Yasukawa, H. (2022). Virtual captive model tests for ship maneuvering based on CFD and MMG model. *Journal of Marine Science and Application, 21*(3), 456–468. https://doi.org/10.1007/s11804-022-00241-9

Fossen, T. I. (2011). *Handbook of Marine Craft Hydrodynamics and Motion Control.* John Wiley & Sons.

Hino, T. (2015). CFD-based captive model tests for ship maneuvering prediction. *Journal of Marine Science and Technology, 20*(4), 685–699. https://doi.org/10.1007/s00773-015-0331-7

International Maritime Organization. (2020). *Reports on Marine Casualties and Incidents.* IMO.

ITTC. (2017). *Recommended Procedures and Guidelines: CFD in Marine Hydrodynamics.* International Towing Tank Conference.

Liu, Y., Yasukawa, H., & Yoshimura, Y. (2018). Evaluation of hydrodynamic derivatives of ships using CFD. *Journal of Marine Science and Technology, 23*(1), 89–104. https://doi.org/10.1007/s00773-017-0496-3

Sutulo, S., & Soares, C. G. (2020). An overview of mathematical models for ship maneuvering. *Ocean Engineering, 198*, 106980. https://doi.org/10.1016/j.oceaneng.2020.106980

Wang, Y. (2017). Development of computerized planar motion carriage system for ship maneuvering tests. *Journal of Hydrodynamics, 29*(4), 623–632. https://doi.org/10.1016/S1001-6058(16)60765-1

Wilson, R. V., & Haffenden, R. (2020). Advances in planar motion mechanism testing for ship maneuvering. *Ocean Engineering, 195*, 106690. https://doi.org/10.1016/j.oceaneng.2019.106690

Yasukawa, H., & Yoshimura, Y. (2015). Introduction of MMG standard method for ship maneuvering predictions. *Journal of Marine Science and Technology, 20*(1), 37–52. https://doi.org/10.1007/s00773-014-0293-y

Yoshimura, Y., & Masumoto, Y. (2012). Hydrodynamic force database with medium high-speed merchant ships including fishing vessels and investigation into a manoeuvring prediction method. *Journal of the Japan Society of Naval Architects and Ocean Engineers, 14*, 63–73. https://doi.org/10.2534/jjasnaoe.14.63